On the Electronic Structure of ScB^+ : Ground and Low-Lying Excited States

APOSTOLOS KALEMOS and ARISTIDES MAVRIDIS

National and Kapodistrian University of Athens, Department of Chemistry, Laboratory of Physical Chemistry, P.O. Box 64004, 157 10 Zografou, Athens-Greece.

Abstract

The electronic structure of the ScB^+ cation has been studied using MRCI (CASSCF + single + double replacements) techniques and large basis sets, (21s16p9d6f/10s5p2d1f) generalized contracted to [7s6p4d3f/4s3p2d1f]. From the manifold of molecular states emanating from the ^3D_g, ^1D_g, ^3F_g atomic states of Sc^+ and the ground ^2P_u state of the B atom, we have analyzed a series of eight low-lying excited states of symmetries $^4\Sigma^-$, $^2\Sigma^+(2)$, $^2\Sigma^-$, $^2\Pi(2)$, and $^2\Delta(2)$, spanning an energy range of about 1 eV. For all states full potential energy curves have been constructed and spectroscopic constants have been extracted via a standard Dunham analysis. The ground $X^4\Sigma^-$ state of ScB^+ traces its ancestry to the $Sc^+(^3D_g;M=+1)+B(^2P_u;M=-1)$ atomic fragments, with a binding energy of 44.9 kcal/mol at R_e=2.160 Å. The binding mode of the $X^4\Sigma^-$ state can be considered as the result of three half bonds, a σ and two π bonds.

List of contents

ADVANCES IN QUANTUM CHEMISTRY, VOLUME 32

0065-3276/99 $30.00

1. Introduction

Compounds containing transition metal atoms are of considerable interest due to their catalytic and other important material properties [1]. The multifaceted and intricate chemistry of the transition metal elements and their cations derives mainly from the many low-lying atomic states [2], which in turn are due to the similarity of nd, (n+1)s, and (n+1)p orbitals both in spatial extension and energy [3]. The high density of states is, of course, responsible for creating unusual binding modes in such systems, imposing at the same time stringent computational conditions if one wishes to examine their properties by ab-initio methods. Therefore, the quantitative examination of molecules containing transition metal atoms forces us to investigate rather simple systems with the purpose of gleaning some insight in their behaviour, particularly their binding mechanisms and dissociation energies.

We have performed ab initio calculations on the diatomic molecule scandium boride cation, ScB^+, determining the electronic structure both of its ground state and of a series of low-lying excited states.

In the last fifteen years, concerning the first and second row elements of the periodic table, the following diatomic molecules containing the Sc atom have been examined by ab initio post–HF methods : ScH [4], ScH^+ [5], $ScHe^+$ [6], ScLi [7], $ScLi^+$ [8], ScN [9], ScN^+ [10], ScN^{2+} [11], ScO [12], ScO^+ [13], ScF [14], and $ScNe^+$ [6]. We see that the ScB^+ (and the ScB) is in obvious omission and the present work intends to fill this gap, while work is in progress on the TiB^+, VB^+ and CrB^+ systems. As far as we know, no experimental data are available on ScB^+.

2. Some technical details

With the purpose of obtaining accurate dissociation energies (D_e) and binding mechanisms for all nine states considered, a method is required that will ensure a balanced description for all states involved, at all nuclear geometries, from equilibrium to dissociation limits. In the present case with five valence (active) electrons, the CASSCF+1+2 (Complete Active Space SCF + single + double replacements = MRCI) method seems to be the most suitable, being at the same time computationally tractable. Although the MRCI method is not size-extensive [15, 16], due to the relative small number of active electrons, the effect on our results is for all practical purposes negligible.

The (reference) CAS space selected is comprised of ten orbital functions, six of which correspond to the valence space of the Sc^+(4s, 3d), and the rest to the valence space of the B atom (2s, 2p). The number of configuration functions (CFs) resulting from distributing five electrons among ten orbitals, ranges from 500 to 800 CFs depending on the symmetry. Although our calculations were performed

under C_{2v} symmetry, all CASSCF wave functions display pure (axial) angular momentum symmetry, i.e., Λ=0, 1 or 2, Σ, Π, and Δ respectively.

Dynamical correlation was extracted mainly by single and double excitations out of the reference CAS-space. To keep the calculations manageable the approach of "internally contracted" CISD was employed (icMRCI) [17]. Thus our largest CI-expansion reached the number of approximately half a million CFs. Despite the fact that on the CI calculations no $C_{\infty v}$ restrictions were imposed, no serious symmetry breaking problems were detected.

The basis set expansion of the metal is the ANO set of Bauschlicher [18] but with the functions of g-symmetry removed : (21s16p9d6f) contracted to [7s6p4d3f]. For the B atom the correlation consistent basis set of Dunning [19], cc-pVTZ, (10s5p2d1f) contracted to[4s3p2d1f], was employed.

Due to the nature of our PECs (*vide infra*) we were forced to use the state-average (SA) technique [20, 21]. Numerical experiments for some of the states performed with-and-without the SA-method around equilibrium geometries, showed that losses in total energies due to the SA approach were less than 1 mh.

All calculations were done with the MOLPRO suite of codes [22] ; around equilibrium geometries and for certain states, our results were also checked by the COLUMBUS [23] code.

3. Atomic States

The Hartree-Fock energies of the Sc and Sc^+ in their ground states are -759.735546 and -759.538831 h, the former being 0.34 mh higher than the numerical HF value [24] ; corresponding valence-CISD (4s3d) energies are -759.777570 and -759.545129 h. The SCF, CISD and valence full-CI energies of the ground ^2P state of the B atom are -24.528098, -24.596634, and -24.598722 h respectively. While our atomic HF calculations display full rotational symmetry, correlated calculations were done under C_{2v} symmetry conditions. Because the excited states of the Sc^+ atom, ^1D_g and ^3F_g, and the first excited ^4P_g state of the B atom are involved in the molecular states studied, the accurate calculation of the corresponding atomic energy separations is obviously of interest.

Table I contrasts relative energies of the relevant atomic states with corresponding experimental values [2]. Notice the good agreement between the calculated and experimental $^4P_g \leftarrow ^2P_u$ energy splitting of the B atom. On the contrary, the calculated separations $^1D_g \leftarrow ^3D_g$ and $^3F_g \leftarrow ^1D_g$ of the Sc^+ atom are not in satisfactory agreement with the experimental results, the largest discrepancy being 0.137 eV ($^3F_g \leftarrow ^1D_g$), due to differential correlation effects [25].

Table I. Theoretical vs Experimental Atomic Energy Separations, ΔE(eV) of Sc^+ and B atoms.

	Sc^+			B
Method/ΔE	$^1D_g \leftarrow {}^3D_g$	$^3F_g \leftarrow {}^1D_g$	$^3F_g \leftarrow {}^3D_g$	$^4P_g \leftarrow {}^2P_u$
SCF	0.470	0.323	0.793	2.091
CISD	0.272	0.431	0.703	3.521
Exp[a]	0.302	0.294	0.596	3.571

[a] Ref. 2, average over M_J values.

4. Results and Discussion

Table II presents total energies, bond lengths and dissociation energies for nine states of Σ, Π and Δ symmetry at CASSCF, icMRCI and icMRCI+Q (icMRCI + Davidson correction) level of theory. Depending on the morphology of the PECs, harmonic frequencies (ω_e) are also given for some of the states. An overall picture of the computed PECs at the icMRCI level is given in Figure 1 ; notice that the energy range in which all nine states are embedded is about 1 eV. In what follows, and for reasons of clarity, we examine each state separately ordering the states according to their symmetry.

Ground, X $^4\Sigma^-$ (1 $^4\Sigma^-$) state. At infinity the wave function is represented by the combination, $\left|X\,^4\Sigma^-\right\rangle \propto \left|4s3d_{xz}2p_y\right\rangle + \left|4s2p_x3d_{yz}\right\rangle$ or in terms of the $Sc^+(^3D_g)$ and $B(^2P_u)$ atomic states,

$$\left|X\,^4\Sigma^-\right\rangle \propto \left|{}^3D_g;M=+1\right\rangle\otimes\left|{}^2P_u;M=-1\right\rangle - \left|{}^3D_g;M=-1\right\rangle\otimes\left|{}^2P_u;M=+1\right\rangle$$

A schematic representation of the binding mechanism is given by the valence-bond-Lewis diagram

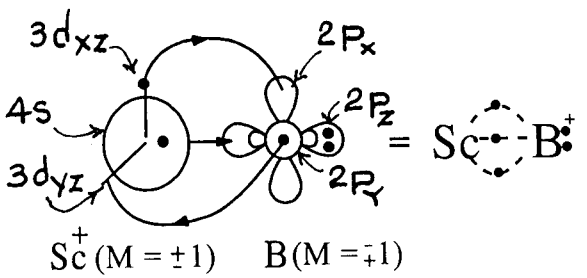

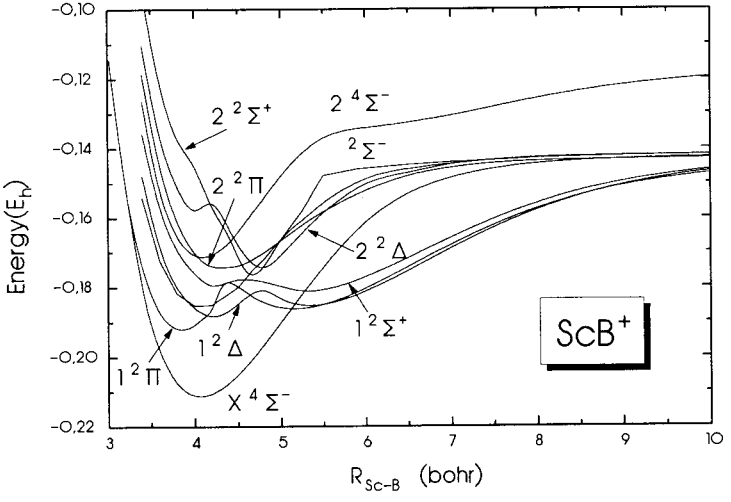

Figure 1. Potential energy curves of ScB^+ at the icMRCI level of theory.

Table II. Energies E(hartree), Bond Distances R_e(Å), Dissociation Energies D_e(kcal/mol), and Harmonic Frequencies ω_e(cm^{-1}) of the $X\,^4\Sigma^-$, $1\,^2\Pi$, $1\,^2\Delta$, $1\,^2\Sigma^-$, $1\,^2\Sigma^+$, $2\,^2\Sigma^+$, $2\,^2\Pi$, $2\,^2\Delta$ and $2\,^4\Sigma^-$ States of ScB^+ in Ascending Energy Order.

State[a]	Method[b,c]	-E	R_e	D_e[d]	ω_e
$X\,^4\Sigma^-$	CASSCF	784.15011	2.181	38.4	452
	icMRCI	784.21000	2.160	44.9	513
	icMRCI+Q	784.213	2.16	45	500
$1\,^2\Pi_{(g)}$	CASSCF	784.14775	2.016	21.6	
	icMRCI	784.19190	2.064	31.5	
	icMRCI+Q	784.194	2.05	32	
$1\,^2\Pi_{(l)}$	CASSCF	784.14307	2.904		
	icMRCI	784.18647	2.737		

(Table II continues)

$1\,^2\Delta_{(g)}$	CASSCF	784.12667	2.211	17.4	
	icMRCI	784.18826	2.233	29.1	
	icMRCI+Q	784.192	2.24	31	
$1\,^2\Delta_{(l)}$	CASSCF	784.13229	2.930		
	icMRCI	784.18528	2.835		
	icMRCI+Q	784.188	2.83		
$1\,^2\Sigma^-$	CASSCF	784.12392	2.109	16.3	
	icMRCI	784.18563	2.167	27.4	
	icMRCI+Q	784.188	2.12	27.6	
$1\,^2\Sigma^+_{(g)}$	CASSCF	784.12697	2.953	17.6	
	icMRCI	784.18118	2.816	24.6	
	icMRCI+Q	784.184	2.80	26	
$1\,^2\Sigma^+_{(l)}$	CASSCF	784.11542	2.206		
	icMRCI	784.17962	2.251		
	icMRCI+Q	784.184	2.26		
$2\,^2\Sigma^+$	CASSCF	784.10716	2.453	5.8	
	icMRCI	784.17682	2.490	21.9	
$2\,^2\Pi$	CASSCF	784.11859	2.280	3.0	
	icMRCI	784.17466	2.293	20.0	438
	icMRCI+Q	784.181	2.28	23	
$2\,^2\Delta$	CASSCF	784.11145	2.483	8.4	
	icMRCI	784.17431	2.532	20.3	
	icMRCI+Q	784.178	2.54	22	
$2\,^4\Sigma^-$	CASSCF	784.11905	2.173	18.9	
	icMRCI	784.17144	2.168	18.1	
	icMRCI+Q	784.174	2.17		

[a] "*g*" and "*l*" refers to "global" and "local" minimum respectively, see text.

[b] With the exception of the $1\,^2\Pi$ state the CASSCF results have been obtained by the state-average method.

[c] +Q refers to Davidson correction for quadruples.

[d] With respect to the ground state products.

which suggests that the two atoms are held together by three-half bonds, one half-σ and two half-π bonds. The CASSCF atomic populations at the equilibrium separation

$$Sc : 4s^{0.28}\ 4p_z^{0.10}\ 3d_\sigma^{0.42}\ 3d_{xz}^{0.56}\ 3d_{yz}^{0.56}$$
$$B\ :\ 2s^{1.52}\ 2p_z^{0.63}\ 2p_x^{0.40}\ 2p_y^{0.40}\ ,$$

clearly corroborate the above picture. The electronic traffic along the reaction coordinate is shown in the evolution population diagram of Figure 2. We observe how the 4s e^- on Sc^+ plummets from 1 e^- at infinity to ~ 0.3 e^- around R_e, the gradual increase of the $2p_z$ e^- on B to ~ 0.6 e-, and the almost symmetric increase and decrease in electron counts of the $d_\pi(Sc^+)$ and $p_\pi(B)$ respectively. Figure 3 shows the $X\ ^4\Sigma^-$ PEC at the CASSCF and icMRCI level of theory. The former captures the chemistry of the system fairly well as is also obvious from the corresponding D_e and R_e values, Table II : At the icMRCI level the D_e increases by less than 7 kcal/mol, with a decrease in bond length by 0.02 Å as compared to the CASSCF values.

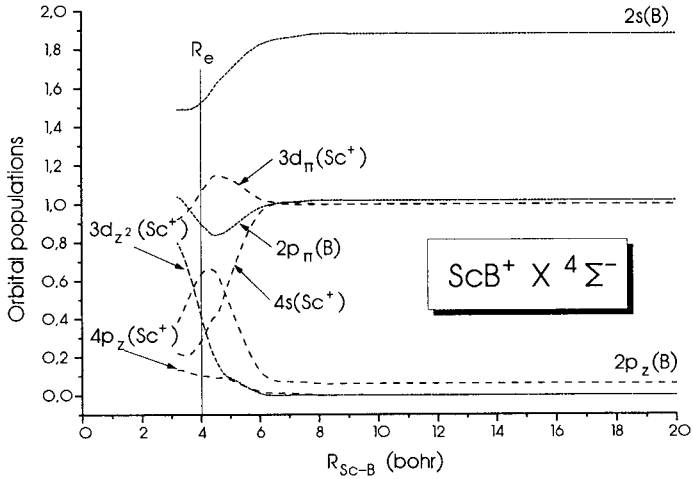

Figure 2. CAS-population evolution diagram of the $X\ ^4\Sigma^-$ state. The perpendicular line R_e refers to equilibrium separation.

$2\,^4\Sigma^-$ state. The binding mode in this state is similar to that of the $X\,^4\Sigma^-$ state, i.e., three-half bonds, one half-σ and two-half π bonds, but the details are entirely different. At infinity the wave function is written as

$$\left|2\,^4\Sigma^-\right\rangle \propto \sqrt{4/5}\left|2p_z 3d_{xz} 3d_{yz}\right\rangle - \sqrt{1/5}\left|2p_z 3d_{x^2-y^2} 3d_{xy}\right\rangle \ ,$$

or in terms of the Sc^+ and B atomic states

$$\left|2\,^4\Sigma^-\right\rangle \propto \left|\,^3F_g; M=0\right\rangle \otimes \left|\,^2P_u; M=0\right\rangle \ .$$

At equilibrium the *in situ* Sc^+ cation finds itself in the excited ~ ^3F state tracing its ancestry there as the PEC shows, Figure 4. A pictorial representation of the wave function at equilibrium, depicting the $\sqrt{4/5}$ component of the function only, is

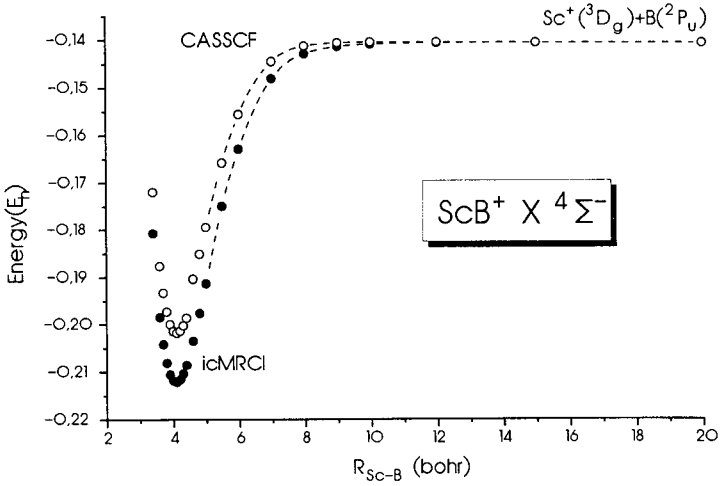

Figure 3. Potential energy curves of the ground $^4\Sigma^-$ state at the CASSCF and icMRCI level of theory.

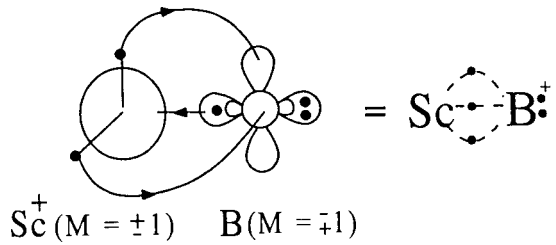

The CAS atomic populations at R_e are

$$Sc : 4s^{0.67}\ 4p_z^{0.10}\ 3d_\sigma^{0.57}\ 3d_{xz}^{0.38}\ 3d_{yz}^{0.38}$$
$$B\ :\ 2s^{1.57}\ 2p_z^{0.08}\ 2p_x^{0.58}\ 2p_y^{0.58}\ ,$$

in agreement with the above icon. Notice the clear formation of the two half-π bonds, the complete transfer of the $2p_z$-boron electron to the metal with the synchronous formation on the latter of a ~ $4s3d_\sigma$ hybrid. Overall we observe a transfer of 1.35 e^- from the B to the Sc^+ atom via the σ-frame with a concomitant "back donation" of 1.16 e^- via the π-frame from the Sc^+ to the B atom. All of these changes along the reaction path are succinctly shown in the evolution population diagram, Figure 5. The bond lengths of the X $^4\Sigma^-$ and 2 $^4\Sigma^-$ states differ by less than 0.01 Å (Table II) which also reflects the bonding similarity between these two states. Now from ~ 5 to 9 bohr the 2 $^4\Sigma^-$ PEC shows a depression, Figure 4, which is probably due to an avoided crossing between the 2 $^4\Sigma^-$ and 3 $^4\Sigma^-$ states. The latter, shown also in Figure 4, has been calculated at the CASSCF level only due to technical difficulties. At the CASSCF level the 3 $^4\Sigma^-$ state is slightly bound; assuming that the binding energy would increase at a higher level of calculation, the 2 $^4\Sigma^-$ – 3 $^4\Sigma^-$ PECs would interact, creating the aforementioned depression in the 2 $^4\Sigma^-$ state.

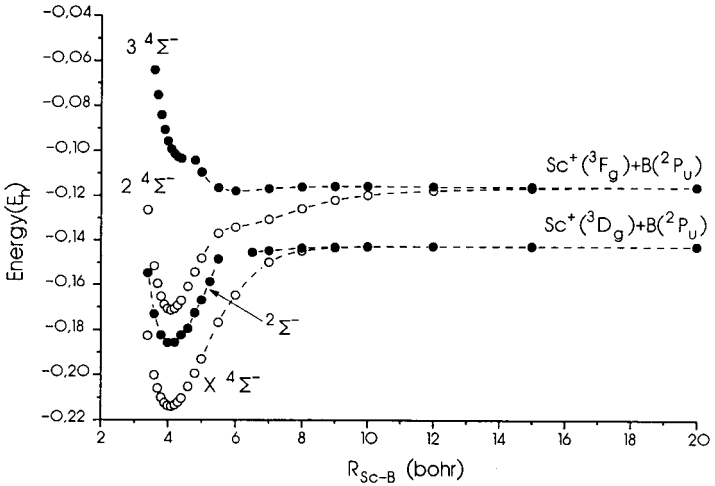

Figure 4. Potential energy curves of Σ^- symmetry states ; the $3\,^4\Sigma^-$ state is at the CASSCF level while the rests at the icMRCI level of theory.

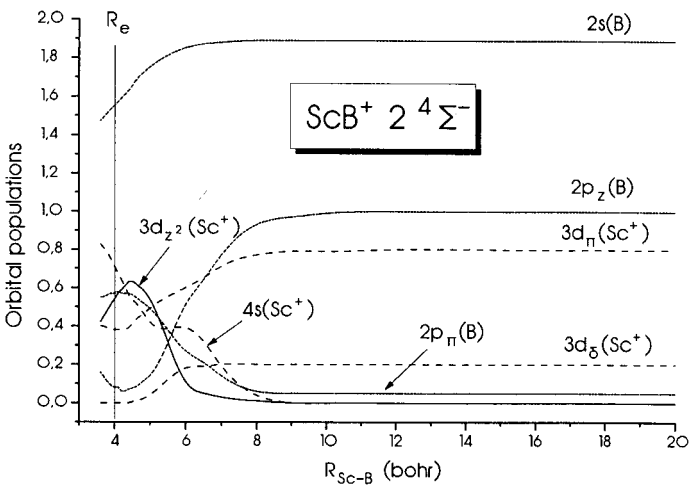

Figure 5. CAS-population evolution diagram of the $2\,^4\Sigma^-$ state.

1 $^2\Pi$ state. As Figure 1 (also see Table II) shows this is the first excited state of the ScB^+ system, being 11.4 kcal/mol above the $X\,^4\Sigma^-$ state at the icMRCI level of theory. The 1 $^2\Pi$ PEC shown in Figure 6 presents two distinct minima, one "global" (*g*) at 3.90 bohr (Table II) and one "local" (*l*) at 5.18 bohr and higher in energy from the first one by ~ 5.5 mh.

Asymptotically we start with $Sc^+(^3D_g\ ;\ M=\pm1) + B(^2P_u\ ;\ M=0)$. As the two atoms approach each other a pure σ-bond is formed by coupling into a singlet the 4s e^- on Sc^+ and the $2p_z$ e^- on the B atom : $|^2\Pi\rangle \propto |(4s3d_\pi)_T 2p_z\rangle$, where the subscript T means "coupled into a triplet". The $3d_{xz}(\pi)$ electron remains strictly localized on the metal, while ~ 0.2 e^- are transferred from B to Sc^+ via the σ-frame. As we move in, passing the *l*-minimum at 5.18 bohr, the *g*-minimum is formed at 3.90 bohr while the bond character changes drastically. The overall reaction, from infinity to *l* to *g* can be represented with the following valence-bond-Lewis pictures

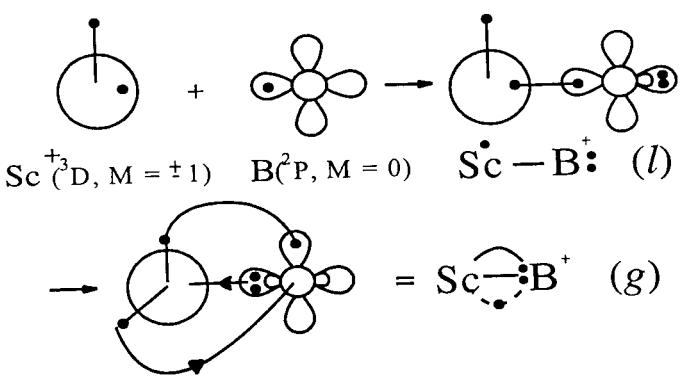

At the *g*-minimum the *in-situ* metal finds itself in the ~ ^3F excited state with M=0, while the B atom has to change its M value to ±1. That is, between the *l*-*g* minima a switching of the M-values occur between the Sc^+ and B atoms. At equilibrium the CASSCF atomic populations of the two minima are as follows

(*l*) $\quad Sc : 4s^{1.08}\ 4p_z^{0.05}\ 3d_\sigma^{0.04}\ 3d_{xz}^{1.0}$

$\quad\quad B : 2s^{1.84}\ 2p_z^{0.84}\ 2p_x^{0.06}\ 2p_y^{0.06}$

(*g*) $\quad Sc : 4s^{0.16}\ 4p_z^{0.10}\ 3d_\sigma^{0.16}\ 3d_{xz}^{0.49}\ 3d_{yz}^{1.05}$

$\quad\quad B : 2s^{1.50}\ 2p_z^{0.06}\ 2p_x^{0.49}\ 2p_y^{0.87}$

As the populations show at the *g*-minimum we have a π-bond, a σ-bond, and a half π-bond from the Sc^+ to the B atom. Also this state has the shortest bond length of all states studied here and the largest intrinsic bond strength, ~ 48 kcal/mol with respect to $Sc^+(^3F_g)$ + $B(^2P_u)$; 0.44 e^- are transferred from B to Sc^+ and ~ 0.5 e^- from Sc^+ to B via the π-frame. It is of interest to mention at this point that we were unable to calculate correctly this 1 $^2\Pi$ state using the COLUMBUS code. As a matter of fact, despite of all our efforts, we obtained two crossing curves of $^2\Pi$ symmetry (Figure 7). The lowest in energy presents a minimum at R_e=3.88 bohr with an energy E=-784.19078 h and correlating to $Sc^+(^3F_g)$ + $B(^2P_u)$, obviously corresponding to the *g* part of the 1 $^2\Pi$ state (Figure 6), while the other one presents its minimum at R_e=5.22 bohr, E=-784.18507 h dissociating to $Sc^+(^3D_g)$+$B(^2P_u)$ corresponding to the (*l*) part of the 1 $^2\Pi$ state. Somehow, and inadvertently, we have constructed the two "diabatic" PECs that give rise to the morphology of the adiabatic 1 $^2\Pi$ curve (Figure 6).

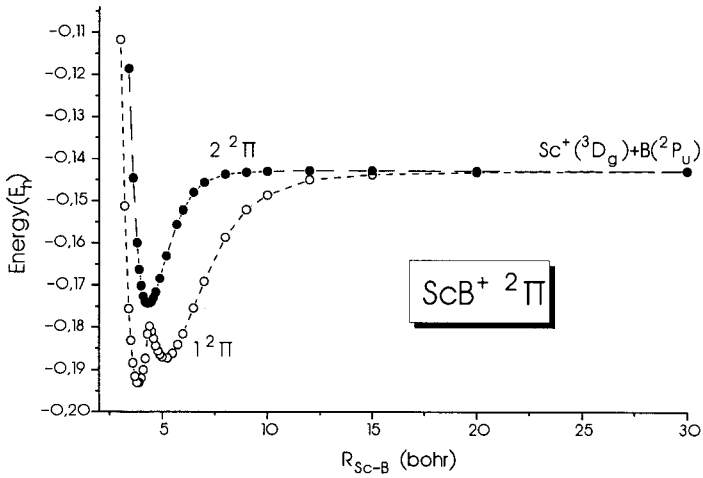

Figure 6. Potential energy curves of the 1 $^2\Pi$ and 2 $^2\Pi$ states at the icMRCI level of theory ; the double well of the 1 $^2\Pi$ is due to an avoided crossing.

The population evolution diagram of the 1 $^2\Pi$ PEC shown in Figure 8 summarizes essentially our conclusions for this state. For instatnce, the 4s orbital on Sc^+ maintains up to 5 bohr, where the *l*-minimum occurs, a constant population of

~ 1 e^-, but around 4 bohr plummets to ~ 0.15 e^- where the *g*-minmum occurs. This situation is similar but more pronounced with the $2p_z$ function on B : it starts asymptotically with 1 e^- and almost retains its population up to the first min, ~ 5 bohr. Passing the 5 bohr point it plummets and its population practically vanishes. The $3d_{xz}$ and $3d_{yz}$ on the metal follow an opposite route, i.e., the former starts from 1 e^- at infinity and ends up at ~ 0.5 e^- around the equilibrium while the latter at infinity is empty, aquiring ~ 1 e^- around the equilibrium.

2 $^2\Pi$ state. The PEC of the 2 $^2\Pi$ state is shown in Figure 6 along with the 1 $^2\Pi$ PEC for reasons of comparison. Notice that both these states correlate to the same asymptotic products, $Sc^+(^3D_g)$ + $B(^2P_u)$. Numerical equilibrium results are presented in Table II. Here, the molecule is created via a half π-bond as the result of electron transfer from B to Sc^+, and a σ-bond as the result of electron transfer along the molecular axis from Sc^+ to B.

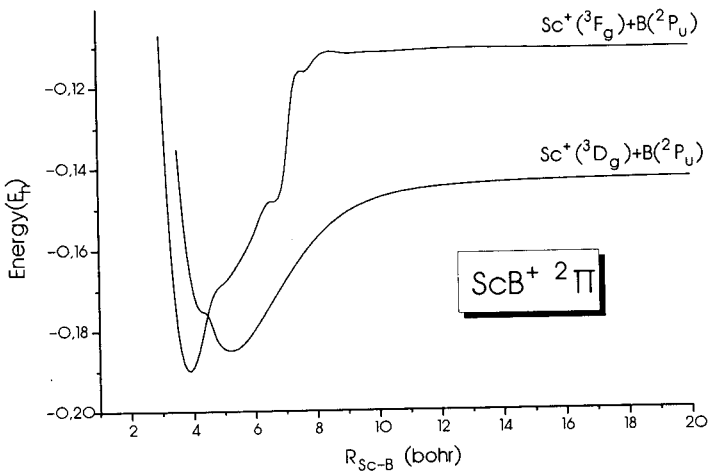

Figure 7. Potential energy curves of $^2\Pi$ symmetry with erroneous crossing. Calculated by the COLUMBUS code at the MRCI level.

We have the following valence-bond-Lewis cartoon

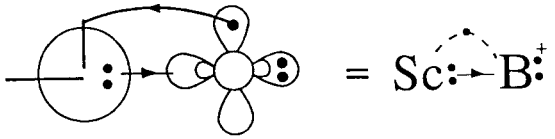

$Sc^{+}(M = 0)$ $B(M = \pm 1)$

with the CASSCF equilibrium populations

$$Sc : 4s^{0.75}\ 4p_z^{0.08}\ 3d_\sigma^{0.77}\ 3d_{xz}^{0.37}$$

$$B : 2s^{1.56}\ 2p_z^{0.67}\ 2p_x^{0.60}\ 2p_y^{0.09}$$

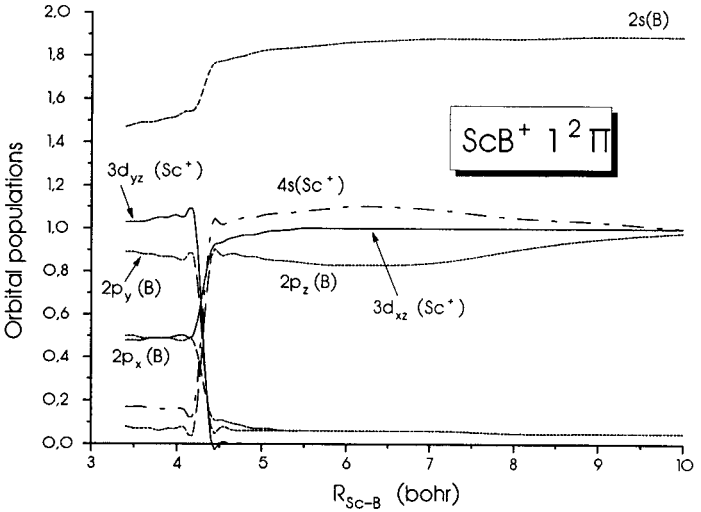

Figure 8. CAS-population evolution diagram of the $1\ ^2\Pi$ state.

Approximately 0.8 e^- are "circling" around, ~ 0.4 e^- from the $2p_x$ of B are trasferred to the $3d_{xz}$ of Sc^+, and ~ 0.4 e^- from the hybrid ~ $4s3d_\sigma$ to the $2p_z$ of B.

1 $^2\Delta$ and 2 $^2\Delta$ states. Figure 9 displays the icMRCI PECs of these two states and Table II the equilibrium numerical results. Asymptotically we start with the metal in its $|^3D_g; M = \pm 2\rangle$ state and with the B atom in the $|^2P_u; M = 0\rangle$ state, i.e., $|^3D_g; M = \pm 2\rangle \otimes |^2P_u; M = 0\rangle$, or in terms of the atomic orbitals, $\sim |(4s3d_\Delta)_T 2p_z\rangle$. As the B moiety moves in with the p_z e^- along the internuclear axis a σ-bond is formed around 5.37 bohr (*l*-minimum) with a d_Δ electron strictly localized, playing no essential rôle in the bonding, but simply carrying the symmetry of the state. Forcing the B atom closer a global (*g*) minimum is formed, with synchronous change in the M values of both atoms, $Sc^+(M=\pm1)$ and B(M=±1) to satisfy the Δ symmetry. Now the two atoms are held together by a π-bond and a half σ-bond. The valence-bond-Lewis icons and the corresponding atomic populations are as follows

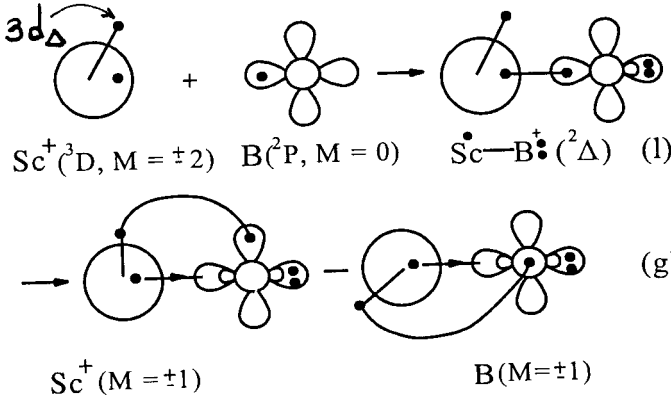

(*l*) $Sc : 4s^{1.06}\ 4p_z^{0.06}\ 3d_\sigma^{0.05}\ 3d_\Delta^{1.00}$

$B : 2s^{1.84}\ 2p_z^{0.86}\ 2p_x^{0.06}\ 2p_y^{0.06}$

(*g*) $Sc : 4s^{0.37}\ 4p_z^{0.08}\ 3d_\sigma^{0.30}\ 3d_{xz}^{0.58}\ 3d_{yz}^{0.58}$

$B : 2s^{1.53}\ 2p_z^{0.67}\ 2p_x^{0.40}\ 2p_y^{0.40}$.

From the "*l*" to the "*g*" minimum, notice the dramatic bond shortening (by ~ 0.6 Å), while the total energy drops by 3 mh (Table II). At this point an observation is pertinent : The $^2\Delta$ has two components, $^2A_1$ and $^2A_2$ under C_{2v} symmetry. At the

g-minimum the $^2A_1$ component can be written as $\sim (|\sigma\pi_x^2\rangle - |\sigma\pi_y^2\rangle)(\alpha\beta - \beta\alpha)\alpha$ and this is shown pictorially in the previous icon. However, the $^2A_2$ component, of course degenerate with the $^2A_1$, can be written as

$$\sim |\sigma\pi_x\pi_y\rangle[0.77(2\alpha\alpha\beta - \alpha\beta\alpha - \beta\alpha\alpha) - 0.45(\alpha\beta - \beta\alpha)\alpha] \ ,$$

This last wave function can be represented pictorially by

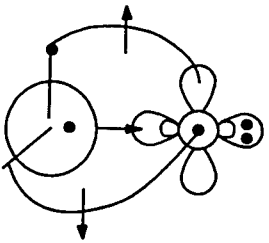

This last picture suggests that we have three half bonds, two π half bonds, from Sc^+ to B and from B to Sc^+ and one σ half bond from Sc^+ to B. The above discussion shows that in molecules of this type an "objective" interpretation of the binding mode is not always plaussible.

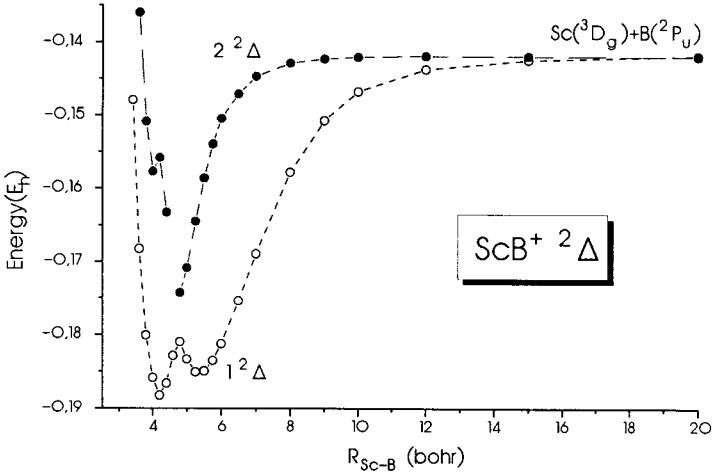

Figure 9. Potential energy curves of $1\ ^2\Delta$ and $2\ ^2\Delta$ states at the icMRCI level presenting avoided crossing.

The asymptote of the $2\ ^2\Delta$ state ($^2A_1$ component) can be written, $|2\ ^2\Delta\rangle \propto |4s(2p_x 3d_{xz})_S\rangle - |4s(2p_y 3d_{yz})_S\rangle$ or in terms of the atomic functions $|2\ ^2\Delta\rangle \propto |\ ^3D_g ; M = \pm 1\rangle \otimes |\ ^2P_u ; M = \pm 1\rangle$, with its PEC shown in Figure 9. Observe a second avoided crossing around the distance of 4 bohr which originates from the ^1D_g state of the Sc^+ atom. At equilibrium this $2\ ^2\Delta$ state can be represented by the wave function $|2\ ^2\Delta\rangle \propto 0.7|(\sigma^2)\sigma^2\delta^1\rangle + 0.4(|\sigma^1\pi_x^2\rangle - |\sigma^1\pi_y^2\rangle)$ with CASSCF populations

$$Sc : 4s^{0.78}\ 4p_z^{0.07}\ 3d_\sigma^{0.13}\ 3d_{xz}^{0.25}\ 3d_{yz}^{0.25}\ 3d_\Delta^{0.60}$$

$$B : 2s^{1.70}\ 2p_z^{0.78}\ 2p_x^{0.21}\ 2p_y^{0.21} \ .$$

The equilibrium bond length, 2.532 Å (Table II) occurs approximately at the average of the *l* and *g* minima of the $1\ ^2\Delta$ state. Overall ~ 0.1 e^- are transferred from B to Sc^+.

$1\ ^2\Sigma^+$ and $2\ ^2\Sigma^+$ states. As Figure 10 shows the $1\ ^2\Sigma^+$ PEC presents two minima as the result of an avoided crossing between the two $^2\Sigma^+$ states, but the first minimum, i.e., the one that appears at longer distance, 5.33 bohr (Table II) is lower in energy by 1.5 mh from the second which occurs at 4.25 bohr. As a matter of fact and within the accuracy of the present methodology these two minima are degenerate. However as before the bonding mechanism from the one to the other is totally different. Observe the schematic valence-bond-Lewis icons.

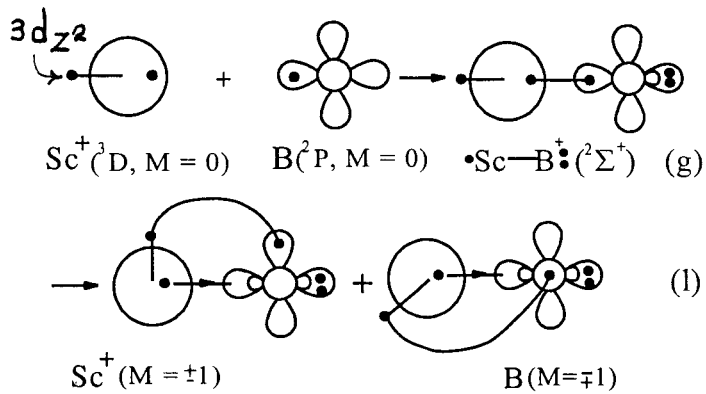

The equilibrium CASSCF populations are

$$(l) \qquad \begin{aligned} &Sc : 4s^{1.09}\ 4p_z^{0.05}\ 3d_\sigma^{1.01} \\ &B\ :\ 2s^{1.85}\ 2p_z^{0.85}\ 2p_x^{0.06}\ 2p_y^{0.06} \end{aligned}$$

$$(g) \qquad \begin{aligned} &Sc : 4s^{0.38}\ 4p_z^{0.08}\ 3d_\sigma^{0.30}\ 3d_{xz}^{0.57}\ 3d_{yz}^{0.57} \\ &B\ :\ 2s^{1.52}\ 2p_z^{0.66}\ 2p_x^{0.41}\ 2p_y^{0.41}\ . \end{aligned}$$

At the first minimum, the "g", both atoms are in their M=0 state ; we have a pure σ-bond, a transfer of ~ 0.2 e^- from B to Sc^+ and a very large bond length. At the "l" minimum, and at a much shorter distance (2.251 Å), both atoms aquire an M=±1 value. The result is a pure π-bond and a half σ-bond from Sc^+ to B. No total charge transfer is observed. This 1 $^2\Sigma^+$ state is $^2A_1$ under C_{2v} symmetry and at equilibrium can be written as ~ $(|\sigma\pi_x^2\rangle + |\sigma\pi_y^2\rangle)(\alpha\beta - \beta\alpha)\alpha$, similar to the 1 $^2\Delta$ ($^2A_1$) but with "+" instead of a "–" sign (*vide supra*).

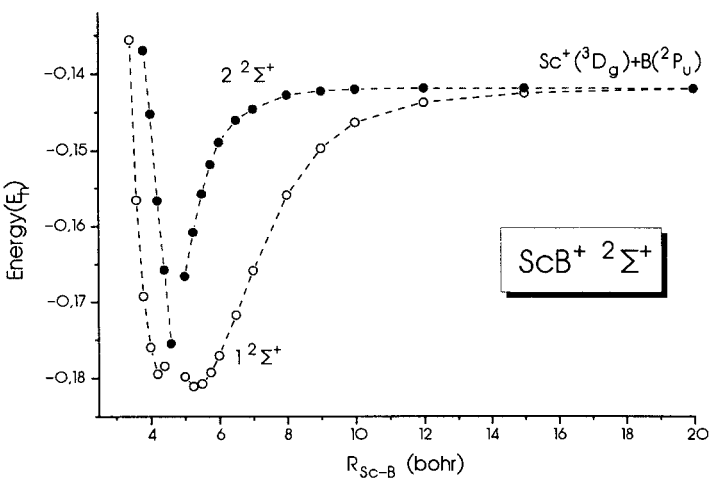

Figure 10. Potential energy curves of 1 $^2\Sigma^+$ and 2 $^2\Sigma^+$ states at the icMRCI level presenting avoided crossing.

The 2 $^2\Sigma^+$ state correlating to the $Sc^+(^3D_g)$ + $B(^2P_u)$ as the 1 $^2\Sigma^+$ (Figure 10), has an asymptotic wave function $|^2\Sigma^+\rangle \propto |4s(2p_x 3d_{xz})_S\rangle + |4s(2p_y 3d_{yz})_S\rangle$ or in terms of the atomic states

$$|^2\Sigma^+\rangle \propto |^3D_g;M=1\rangle \otimes |^2P_u;M=-1\rangle + |^3D_g;M=-1\rangle \otimes |^2P_u;M=1\rangle.$$

The molecule is formed through a π-bond and a half σ-bond as the following icon indicates and the equilibrium CASSCF populations corroborate.

$$Sc: 4s^{0.62}\ 4p_z^{0.06}\ 3d_\sigma^{0.17}\ 3d_{xz}^{0.56}\ 3d_{yz}^{0.56}$$
$$B: 2s^{1.62}\ 2p_z^{0.53}\ 2p_x^{0.41}\ 2p_y^{0.41}\ .$$

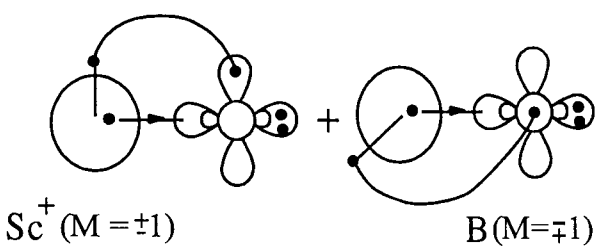

No net charge transfer is observed.

1 $^2\Sigma^-$ state. This is exactly similar to the X $^4\Sigma^-$ state but with one spin flip to form the doublet. The asymptotic wave function and the valence-bond-Lewis icon are identical with that of the X $^4\Sigma^-$ state. The binding mechanism is also similar with that of the X $^4\Sigma^-$ state, i.e., it comprises of two half π-bonds and a half σ-bond. This is clear from the equilibrium CASSCF atomic populations

$$Sc: 4s^{0.20}\ 4p_z^{0.12}\ 3d_\sigma^{0.52}\ 3d_{xz}^{0.55}\ 3d_{yz}^{0.55}$$
$$B: 2s^{1.55}\ 2p_z^{0.56}\ 2p_x^{0.41}\ 2p_y^{0.41}\ ,$$

which are practically the same with the populations of the X $^4\Sigma^-$ state. Figure 4 shows the 1 $^2\Sigma^-$ PEC, as well as the X $^4\Sigma^-$ PEC for reasons of comparison ; at the icMRCI level the bond distance (Table II) between the two states differ by

0.015 Å, again indicating the similarity of the states. At equilibrium the wave function of the $1^2\Sigma^-$ ($^2A_2$) state can be written as

$$\sim \left|\sigma\pi_x\pi_y\right\rangle [0.77\,(2\alpha\alpha\beta - \alpha\beta\alpha - \beta\alpha\alpha) + 0.45(\alpha\beta - \beta\alpha)\alpha]$$

which differs from the $^2A_2$ component of the $^2\Delta$ state in the sign of the spin function, "+" here, "–" in the $^2\Delta$ state (*vide supra*). Notice finally the kink in the $1\ ^2\Sigma^-$ PEC around 5 bohr, Figure 4 ; the cause of this is shown in Figure 11. This last figure presents the $1\ ^2\Sigma^-$ and $2\ ^2\Sigma^-$ PECs at the CASSCF level of theory only. It is obvious that the kink of the $1\ ^2\Sigma^-$ PEC is due to an avoided crossing between a repulsive $^2\Sigma^-$ state correlating to $Sc^+(^3D_g) + B(^2P_u)$ and the $2\ ^2\Sigma^-$ which traces its ancestry to $Sc^+(^1D_g) + B(^2P_u)$. We have another avoided crossing between the repulsive $2\ ^2\Sigma^-$ PEC and the $3\ ^2\Sigma^-$ PEC which correlates to $Sc^+(^3F_g) + B(^2P_u)$. As previously mentioned we were unable to calculate the $2\ ^2\Sigma^-$ PEC at the icMRCI level because of technical reasons.

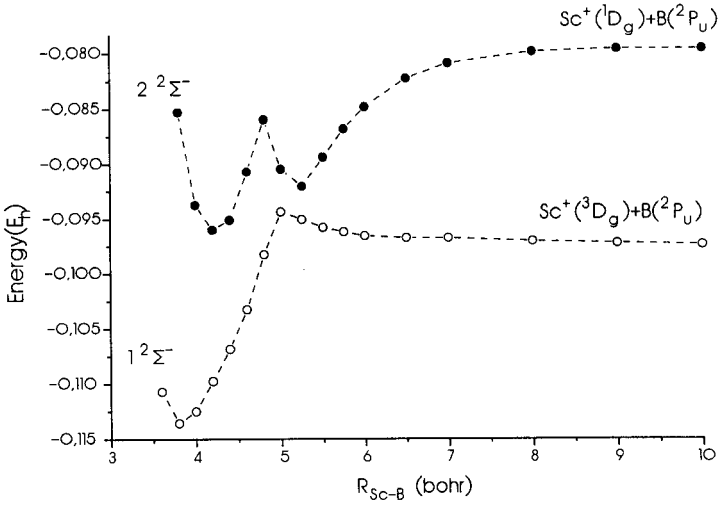

Figure 11. Potential energy curves of $1\ ^2\Sigma^-$ and $2\ ^2\Sigma^-$ states at the CASSCF level.

5. Synopsis and final remarks

At the icMRCI level of theory we have calculated full PECs for nine states of the scandium boride cation, ScB^+. The symmetry of the ground state is $^4\Sigma^-$ with a bond distance of 2.160 Å and a binding energy of 44.9 kcal/mol. We believe that the first excited state is of $^2\Pi$ symmetry, ~ 11.5 kcal/mol above the X $^4\Sigma^-$ state. Table III presents a summary of D_e's, R_e's of all states, as well as, their binding mechanism in a schematic way by employing simple Lewis-like pictures. It is worth emphasizing the following points

1. A very large number of bound states is packed in a short, ~ 1 eV, energy range. Some of the states are essentially degenerate within the accuracy of our calculations ; for instance the 2 $^2\Pi$ and 2 $^2\Delta$ states differ by ~ 0.5 mh, Tables II and III.

2. We have a variety of binding schemes (codified in Table III) ranging from three half-bonds to simple σ-bonds.

3. In the states 1 $^2\Sigma^+_g$, 1 $^2\Delta_l$ and $^2\Pi_l$, where the molecule is held together by a pure σ-bond, the binding energy is practically the same for all three states, ranging from 25 to 28 kcal/mol.

4. Bond lengths vary significantly from state-to-state, the shorter and larger bond distances being 2.064 (1 $^2\Pi_g$) and 2.835 (1 $^2\Delta_l$) Å.

5. During bond formation and for the states 2 $^4\Sigma^-$, 2 $^2\Delta$, 1 $^2\Sigma^+$ about 0.2 e^- are transferred from B to Sc^+, for the rest of the states no significant charge movement occurs.

6. Due to avoided crossings the PECs of the states 1 $^2\Pi$, 1 $^2\Delta$ and 1 $^2\Sigma^+$ present double minima characterized formally as "*g*" and "*l*", global and local respectively. Due to very small energy barriers between the *g* and *l* minima bond distances for these states are not well defined. This is particularly obvious in the state 1 $^2\Sigma^+$, Figure 10, where the energy barrier between the two minima is ~ 1 mh.

7. All our MRCI calculations are size extensive within 0.5 mh.

Table III. Summary of "Schematic" Binding Modes, Bond Distances R_e(Å), and Dissociation Energies D_e(kcal/mol), of the Ground ($X\ ^4\Sigma^-$) and Eight Low-Lying States in Ascending Energy Order of ScB^+, and at the icMRCI level of theory.

State[a]	Binding Mode[b]	R_e	D_e[c]
$X\ ^4\Sigma^-$	Sc⋮B:	2.160	44.9
$1\ ^2\Pi_{(g)}$	Sc⋮B	2.064	31.5
$1\ ^2\Pi_{(l)}$	Sc —B:	2.737	
$1\ ^2\Delta_{(g)}$	Sc⋮B:	2.233	29.1
$1\ ^2\Delta_{(l)}$	Sc —B:	2.835	
$^2\Sigma^-$	Sc⋮B:	2.167	27.4
$1\ ^2\Sigma^+_{(g)}$	Sc— B:	2.816	24.6
$1\ ^2\Sigma^+_{(l)}$	Sc⋮B:	2.251	
$2\ ^2\Sigma^+$	Sc⋮B:	2.490	21.9
$2\ ^2\Pi$	Sc⋮B:	2.293	20.0
$2\ ^2\Delta$		2.532	20.3
$2\ ^4\Sigma^-$	Sc⋮B:	2.168	18.1

[a] *g* and *l* refer to "global" and "local" min, see text.

[b] Bend lines represent π-bonds, straight lines represent σ-bonds, while dashed lines with a dot represent half bonds.

[c] All D_e's are with respect to the ground state products.

References

[1] N. N. Greenwood and A. Earnshaw, *Chemistry of the Elements*, Pergamon Press, Oxford (1984)

[2] C. E. Moore, *Atomic Energy Levels*, NSRDS-NBS Cirular No. 35, Washington, D. C. (1971)

[3] S. R. Langhoff and C. W. Bauschlicher, Jr., Ann. Rev. Phys. Chem. **39**, 213 (1988)

[4] C. W. Bauschlicher, Jr., and S. P. Walch, J. Chem. Phys. **76**, 4560 (1982)

[5] A. E. Alvarado-Swaisgood and J. F. Harrison, J. Phys. Chem. **89**, 5198 (1985)
[6] H. Partridge, C. W. Bauschlicher, Jr., and S. R. Langhoff, J. Phys. Chem. **96**, 5350 (1992)
[7] J. F. Harrison, J. Phys. Chem. **87**, 1323 (1983)
[8] D. B. Lawson and J. F. Harrison, J. Phys. Chem. **100**, 6081 (1996)
[9] K. L. Kunze and J. F. Harrison, J. Am. Chem. Soc. **112**, 3812 (1990)
[10] K. L. Kunze and J. F. Harrison, J. Phys. Chem. **93**, 2983 (1989)
[11] K. L. Kunze and J. F. Harrison, J. Phys. Chem. **95**, 6418 (1991)
[12] C. W. Bauschlicher, Jr., and P. Maitre, Theor. Chim. Acta **90**, 189 (1995)
[13] J. L. Tilson and J. F. Harrison, J. Phys. Chem. **95**, 5097 (1991)
[14] J. F. Harrison, J. Phys. Chem. **87**, 1312 (1983)
[15] R. J. Bartlett, Annu. Rev. Phys. Cnem. **32**, 359 (1981)
[16] W. Duch and G. H. F. Diercksen, J. Chem. Phys. **101**, 3018 (1994)
[17] H.-J. Werner and P. J. Knowles, J. Chem. Phys. **89**, 5803 (1988) ; P. J. Knowles and H.-J. Werner, Chem. Phys. Lett. **145**, 514 (1988) ; H.-J. Werner and E. A. Reinsch, J. Chem. Phys. **76**, 3144 (1982) ; H.-J. Werner, Adv. Chem. Phys. **LXIX**, 1 (1987)
[18] C. W. Bauschlicher, Jr., Theor. Chim. Acta **92**, 183 (1995)
[19] T. H. Dunning, Jr., J. Chem. Phys. **90**, 1007 (1989)
[20] K. Docken and J. Hinze, J. Chem. Phys. **57**, 4928 (1972)
[21] H.-J. Werner and W. Meyer, J. Chem. Phys. **74**, 5794 (1981)
[22] MOLPRO is a package of *ab initio* programs written by H.-J. Werner and P. J. Knowles, with contributions from J. Almlof, R. D. Amos, A. Berning, M. J. O. Deegan, F. Eckert, S. T. Elbert, C. Hambel, R. Lindh, W. Meyer, A. Nicklass, K. Peterson, R. Pitzer, A.J. Stone, P. R. Taylor, M. E. Mura, P. Pulay, M. Schuetz, H. Stoll, T. Thorsteinsson, and D. L. Cooper.
[23] R. Shepard, I. Shavitt, R. M. Pitzer, D. C. Comeau, M. Pepper, H. Lischka, P. G. Szalay, R. Ahlrichs, F. B. Brown and J.-G. Zhao, Intern. J. Quantum Chem. **S22**, 149 (1988)
[24] P. J. Hay, J. Chem. Phys. **66**, 4377 (1977)
[25] B. H. Botch, T. H. Dunning, Jr., and J. F. Harrison, J. Chem. Phys. **75**, 3466 (1981)